A Miniature Quadrifilar Helix Antenna for Global Positioning Satellite Reception

Yu-Shin Wang and Shyh-Jong Chung, *Senior Member, IEEE*

***Abstract*—The design is described of a very compact quadrifilar helix antenna. A hollow ceramic rod is used as a dielectric load to reduce antenna size, which is only 2.7% of an air-loaded quadrifilar helix antenna. A simple equivalent circuit is established for the proposed quadrifilar helix antenna to demonstrate impedance characteristics. A self-phasing method for achieving circular polarization is also proposed. This method is convenient for tuning circular polarization. Additionally, a compact matching structure is designed to match the proposed antenna, which only utilizes short transmission-line sections and one capacitor. For experiments, the proposed antenna is designed at 1.575 GHz such that it can be utilized for global position system. Measurement and simulation results agree. A hemispherical pattern with a beamwidth of 150° is measured. This circular-polarized pattern with a wide beamwidth is feasible for mobile applications.**

***Index Terms*—Circular polarization, GPS, quadrifilar helix antenna (QHA), self phasing.**

I. Introduction

THE resonant quadrifilar helix antenna (QHA) can generate a hemispherical radiation pattern for circular polarization. This radiation pattern with a wide beamwidth can facilitate low-elevation reception or a wide angular receiving range. This antenna is already applied in many spacecraft systems [1]. The advantages of the hemispherical radiation pattern of the QHA are also attractive for mobile satellite communication and position-location systems, which typically require circular polarization and a wide beamwidth. The conventional resonant QHA has two resonant bifilar helix antennas (BHAs) oriented in a mutually orthogonal relationship on a common axis. The resonant BHA can be treated as a twisted one-wave-length loop antenna. To achieve circular polarization, these two BHAs are fed in quadrature phase. The radiation pattern shape of the resonant QHA depends on helix dimensions, number of turns and pitch angle. When four arms are roughly half wavelength with half turn with axial length equal to a quarter wavelength, the radiation pattern approaches a hemisphere like a cardioidal shape [2].

Manuscript received April 22, 2008; revised February 07, 2009. First published June 02, 2009; current version published December 01, 2009.

Y.-S. Wang is with Teradyne, Inc., Hsinchu, Taiwan 302, R.O.C.

S. J. Chung is with the Department of Communication Engineering, National Chiao Tung University, Hsinchu, Taiwan, R.O.C. (e-mail: jchung@cm.nctu.edu.tw).

Color versions of one or more of the figures in this paper are available online at http://ieeexplore.ieee.org.

Digital Object Identifier 10.1109/TAP.2009.2024132

The demand for global positioning systems (GPSs) has recently grown dramatically for portable tracking devices or mobile phones with GPS functions. This need has led to the increased requirement for circular-polarized antennas. The good radiation property of resonant QHAs has drawn considerable attention. However, the half wavelength of 1.575 GHz (GPS L_1 frequency) for a resonant QHA is too long to be integrated into handsets without minimizing the QHA.

Several methods for modifying QHAs have been proposed, including miniaturization. In [3], the inserted open stubs have been employed to miniaturize a QHA. A QHA printed on flexible substrate increases design flexibility. Many studies have investigated for printed QHAs. For example, the helical arms can be shaped easily for bandwidth improvement or miniaturization [4], [5]. In [6], the meander lines were printed on a flexible dielectric film to reduce antenna size. Printed QHAs can also be integrated easily with a hybrid circuit for phase quadrature excitation [7]. Nevertheless, most of printed QHA are not sufficiently small for use in handsets. In [8]–[11], a dielectric-loaded QHA with balun integration is compact. It has a small antenna impedance of 2 Ω with radiation efficiency of 25% [10]. However, use of a low-impedance quarter-wavelength coaxial cable for matching increases fabrication cost and complexity. In [12], a miniaturized balun transformer is designed to feed a dielectric-loaded QHA and achieve impedance matching simultaneously. This work presents a miniature dielectric-loaded resonant QHA, which is a suitable way of miniaturizing an antenna without changing its geometry such that the radiation pattern is degraded. A ceramic rod is used due to its low loss and high permittivity. The scaled-down size depends on dielectric permittivity. The proposed antenna is only 2.7% of a air-loaded resonant QHA in volume, and is smaller than the antenna in [8].

II. Antenna Configuration

Fig. 1 presents the geometry of the proposed antenna. The overall structure contains a hollow ceramic rod with printed metal strips on the surface and a planar circuit substrate with a matching structure and feeding lines. The ceramic rod with a relative permittivity of 40 helps reduce antenna size. Its low material loss with loss tangent lower than 0.0001 at the frequency under 5 GHz also helps maintain the antenna efficiency. The hollow structure of the rod is designed for fabrication convenience and to retain structure strength. The circuit substrate, which has a protrusion, can be inserted into the ceramic rod during assembly. The metal strips on the ceramic rod surface are silver ensuring good conduction, and are printed by using the low-cost screen-printing technique. To reduce the procedure of manufacture, only the rod sidewall and bottom are printed.

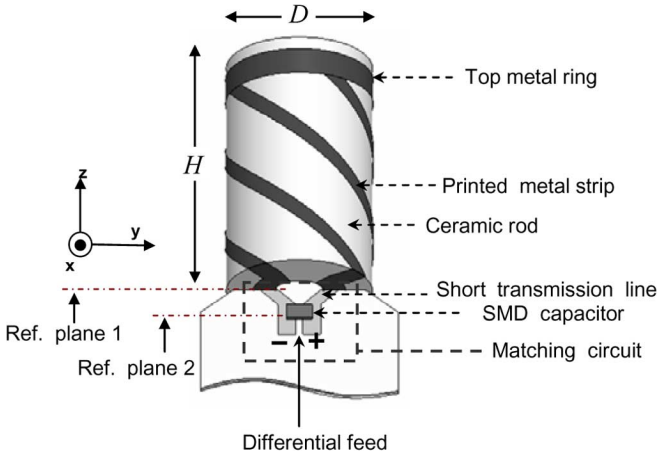

Fig. 1. Antenna structure including the adapted PCB with a SMD capacitor. The antenna dimension is $H = 14.8$ mm and $D = 9$ mm.

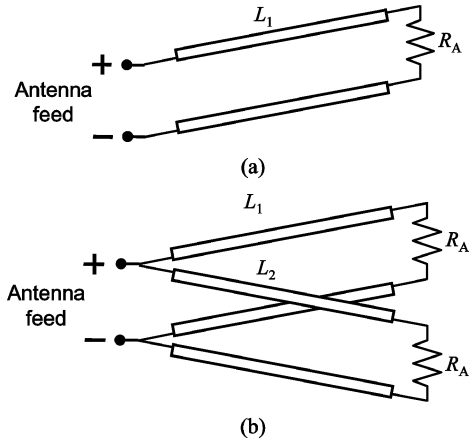

Fig. 2. (a) The equivalent circuit of the proposed BHA. (b) The equivalent circuit of the proposed QHA.

A metal ring on the top of the sidewall is used to connect the four helical arms of the resonant QHA. The feeding lines are a differential line that directly contacts antenna feed points on the ceramic rod bottom. Feeding lines are printed on the circuit substrate. The proposed antenna is designed to operate at 1.575 GHz for GPS applications. The structure is simulated using the full-wave simulation tool, Ansoft HFSS. Due to the high permittivity of the ceramic rod, the antenna is very small, only $D = 9$ mm in diameter and $H = 14.8$ mm in height ($< 0.08\lambda_0$). The hollow-hole diameter in the ceramic rod is 3 mm. The metal strip width is 1 mm. The helical arms are roughly half turns with a pitch length of 22 mm. The helical sense of the antenna affects radiation performance. The helical arms of the antenna are designed in left hand to optimize the right-hand circular polarization (RHCP) gain in the upper half space. This helix sense generates better RHCP gain in the upper space than a left-handed circular polarization (LHCP) gain in the lower space [2].

The remainder of this paper is organized as follows. Section III describes the equivalent circuit and matching network of the proposed QHA. The antenna is matched to 100 Ω by the matching structure. The 100-Ω differential line is then used to feed the antenna. Both the feeding line and matching structure are printed on an 0.8-mm-thick FR4 substrate. The self-phasing method for achieving circular polarization is discussed in Section IV. Measurement results are given is Section V. Section VI presents conclusions.

III. Equivalent Circuit and Matching Network

The impedance characteristics of the dielectric-loaded QHA can be observed from simple equivalent circuits. Fig. 2 presents both equivalent circuits for the BHA and QHA. Because the configuration of BHA is constructed as a twisted pair line, the BHA model consists of a differential transmission line and resistor [Fig. 2(a)]. The characteristic impedance of the transmission line in the model is approximately 65 Ω. This value is similar to the simulated characteristic impedance of the twisted line in a BHA. The resistor includes the effects of radiation resistance and ohm resistance, whose value equals 1.3 Ω (obtained by curve fitting compared with full -wave simulation.) The high permittivity of the ceramic rod makes the antenna very small as compared with the wavelength in free space, and decreases radiation resistance dramatically. The small radiation resistance means that the loss tangent of the ceramic rod becomes very critical to antenna efficiency.

A resonant QHA can be considered as two resonant BHAs arranged orthogonally with quadrature-phase excitation. To simplify the feeding network, the phase quadrature is obtained using the self-phasing method such that only one set of feeding lines is required. By this method, the two BHAs are fed in parallel [see Fig. 2(b)], with one BHA slightly larger than the other. In the proposed design, the electrical lengths L_1 and L_2 of the equivalent transmission line of the two BHAs are 180.8° and 179.2° at the QHA resonant frequency, what are inductive and capacitive, respectively, and cancel each other at the center frequency. The very small difference in length required to achieve circular polarization is based on the small input resistance of the antenna. To compare the full-wave simulation result with the equivalent circuit model, the input impedance of the un-matched antenna was de-embedded to eliminate parasitic inductance from feeding lines. Fig. 3 plots the calculated input impedances of the BHA and QHA from equivalent circuits, and the input impedance of QHA from full-wave simulation, where the reference plane is set as reference plane 1 (Fig. 1). The calculated result for the circuit model agrees with the full-wave simulation, and the impedance of the QHA equals that of the two BHAs connected in parallel. Near the center frequency of the QHA, the impedance curve of an imaginary part becomes flat and the curve of the real part reaches a maximum. The corresponding Smith chart has a tip on the impedance curve around center frequency, as is observed later.

The small input resistance is a critical problem when feeding the proposed antenna. To transform a very small resistance to 100 Ω, the efficiency of the matching circuit should be considered. Furthermore, the matching circuit should also be small such that the entire antenna is compact. Fig. 4 shows the proposed matching circuit, in which two inductors and a capacitor are used to match antenna resistance R_A of 1.3 Ω at the center frequency. To transform the small resistance to 100 Ω, the required value of the inductors and capacitor are $L_S = 0.6$ nH and

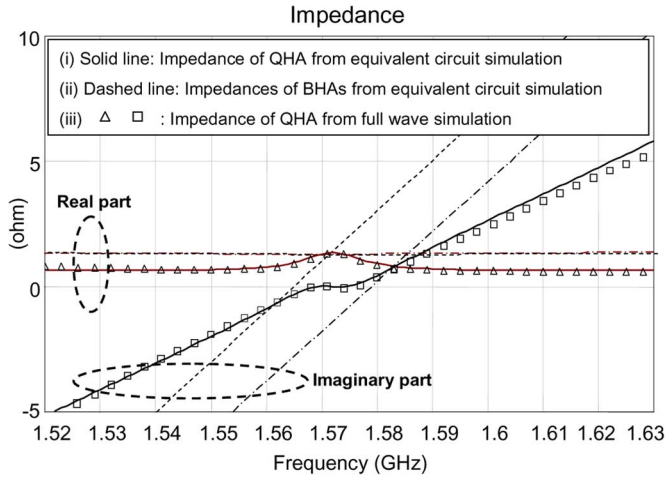

Fig. 3. Impedances from full-wave simulation and equivalent circuit simulation. Noticed that the imaginary parts of the two BHAs are separate, showing different resonant frequencies, and the corresponding real parts coincide with each other with a small resistance of 1.3 Ω.

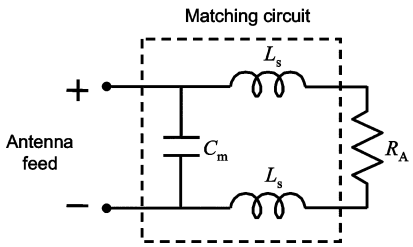

Fig. 4. Schematic diagram of the matching circuit $C_{\rm m} = 8.5$ pF and $L_{\rm S} = 0.6$ nH.

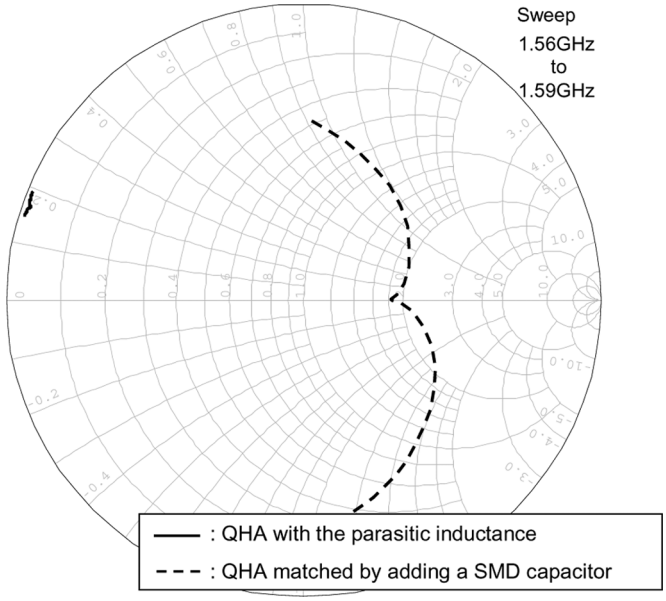

Fig. 5. The simulated input impedance of the antenna at reference plane 2. The solid line represents the antenna without the capacitor. The dashed line represents the antenna matched by adding the capacitor, $C_{\rm m} = 8.5$ pF.

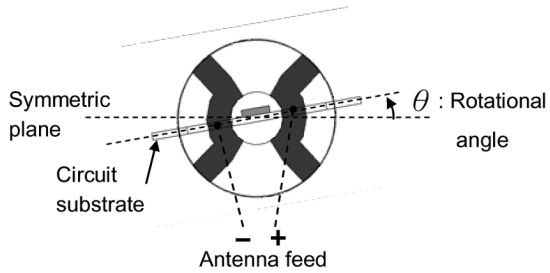

Fig. 6. Bottom view of the QHA of Fig. 1 showing the differential feed points with rotation angle θ, which is adjusted to obtain circular polarization.

$C_{\rm m} = 8.5$ pF, respectively. Notably, a small inductor is utilized, which helps reduce loss and thereby increase the efficiency of the matching network. In practice, the two small inductors are implemented using two parasitic short sections of transmission lines. The large capacitor used is a surface mount device (SMD) component. The capacitor is shunted with feeding lines. Fig. 1 presents the layout of the proposed matching configuration. The circuit size is very small and only one SMD component is used. By appropriately positioning the capacitor, the required length of the short matching transmission-line sections and, thus, the matching inductance can be obtained.

Fig. 5 shows the simulated input impedances of the antenna, with and without the matching capacitor, at reference plane 2 (Fig. 1). Without the matching capacitor, the input impedance is near 1.3 Ω with a small inductive reactance provided by the short transmission line sections from reference plan 1 to 2 (Fig. 1). After adding the capacitor, the impedance can be matched to 100 Ω at the center frequency.

Matching circuit efficiency depends on the loss of components. Since the loss of a short transmission line section is quite low, it can be ignored. The parasitic resistor of the SMD capacitor is of greatest concern. According to the capacitor model from the Murata library [13], the parasitic resistance associated with an 8.5 pF capacitor is 0.33 Ω. The matching efficiency is at least 80%. To increase efficiency further, the single 8.5 pF capacitor can be replaced by two shunt 4.25 pF capacitors.

IV. Self-Phasing Method

In this work, a good RHCP pattern in the upper half space is designed. Fig. 6 presents the method used to attain self-phased quadrature excitation for RHCP. Two feed points are connected to the feeding lines on a circuit substrate for a differential input signal. The circuit substrate is rotated by a small degree, θ, relative to the symmetric plane. After rotation, the lengths of two BHAs become different; this difference proportional to the rotational angle (Fig. 6). However, average length of two BHAs remains the same, implying that resonant frequency will not change because the resonant frequency of a QHA depends on average length of the two BHAs. Rotation makes the length of one BHA longer than the average length and the other shorter. The longer BHA exhibits an inductive impedance at the center frequency and the shorter BHA shows capacitive impedance, which provides the required quadrature-phase excitation for circular polarization. To obtain the RHCP in the upper half space, θ should be positive; otherwise, a negative θ causes LHCP in the upper half space and RHCP in the lower half space.

A set of simulations for different rotational angles was conducted to identify a suitable θ for good circular polarization. Fig. 7 presents simulation results; the frequency responses of

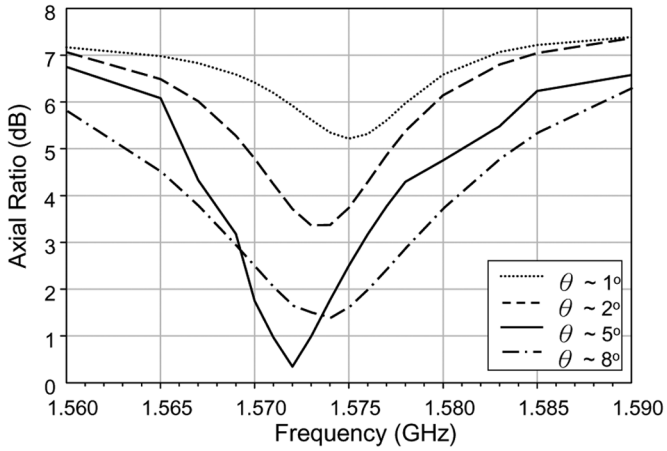

Fig. 7. The simulated axial ratio compared with different rotational angles.

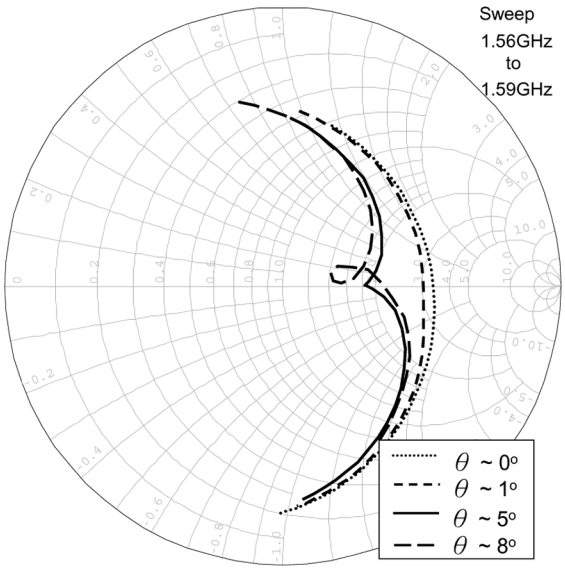

Fig. 8. The simulated impedances with different rotational angles.

the axial ratio for θ from 1–8° are shown. The circular polarization improves when the rotational angle approaches 5°, and then worsens as the angle is increased further. Although not shown, the simulated axial ratios for $\theta = 0°$ are large (30–40 dB), meaning that the radiation field is primarily linearly polarized. Notably, the 3-dB axial ratio bandwidth when $\theta = 8°$ is wider than that when $\theta = 5°$; however, $\theta = 5°$ has the best axial ratio at the center frequency. Fig. 8 shows the variation of impedance for different rotational angles. Since the impedance before matching is quite small, the simulations include the effect of the matching circuit on the substrate for enhanced observation. When θ is around 5°, the minimum axial ratio is achieved, and the circular polarization occurs at the tip (1.572 GHz) of the Smith chart. When θ exceeds 5°, a circle instead of a tip occurs on the impedance curve. The formation of the tip is observed when checking the self-phasing state.

The input impedance bandwidth of the proposed antenna is determined by the matching structure. By using the matching circuit, the simulated 10-dB return-loss bandwidth for $\theta = 5°$ is 12 MHz, which is wider than the corresponding 3-dB axial-ratio

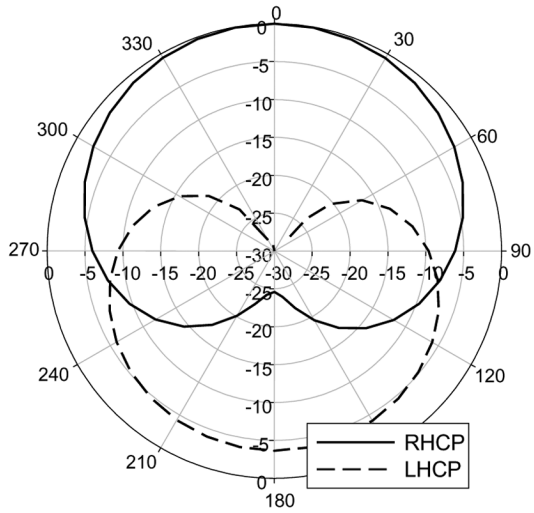

Fig. 9. The simulated radiation pattern when rotational angle is 5°.

bandwidth (7 MHz). Both the small impedance and axial-ratio bandwidths result from the small antenna resistance. Nevertheless, both the bandwidths are sufficient for application on the GPS L1 band. Fig. 9 shows the normalized simulation radiation pattern at the center frequency. The directivity of RHCP is calculated as 2.7 dBic. A good hemispherical circular polarized pattern is obtained, which has a 3-dB beamwidth as wide as 130°. The good cardioid-shaped radiation pattern demonstrates that the overlapping region of two BHAs with a top metal ring does not influence radiation performance. The proposed structure has a radiation pattern similar to that of the conventional resonant QHA. Additionally, Fig. 9 shows both the RHCP pattern and LHCP pattern. The RHCP gain in the upper space is 4 dB higher than the LHCP gain in the lower space, due to the helix design of left-handed sense [2]. Although this front-to-back gain ratio can be further increased by optimizing the helical arms, it suffers from the tradeoff with good hemispherical radiation pattern.

Fig. 10 plots the simulated current distribution of the QHA at 1.572 GHz. The current distribution of each BHA is one-wavelength resonance, just like a loop antenna. At the center frequency, where circular polarization occurs, the two BHAs resonate in phase quadrature as predicted. The closed loop resonance for each BHA is accomplished using the top metal ring.

V. Experimental Results

The proposed antenna was fabricated for experimental investigation. The antenna is fixed to the circuit board via the protrusion. A microstrip balun with 2:1 impedance transformation provides the differential signal. The SMD capacitor used for impedance matching is a Murata GRM1885C1H6R8DZ01. As mentioned, the impedance-matching inductors are realized by two short microstrip-line sections, whose lengths are determined by the shunt capacitor location. By properly tuning the capacitor position, the return loss of the antenna matched better than 10 dB at the center frequency.

Fig. 11 presents the measured input impedances with rotational angles of 0°, 4°, and 8°. The condition of $\theta = 0°$ indicates that the two BHAs are the same length and the corre-

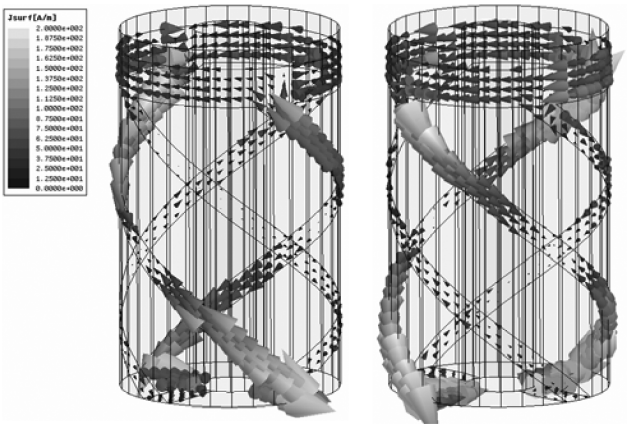

Fig. 10. The current distribution of the proposed antenna with input phases of (a) 0° and (b) 90°.

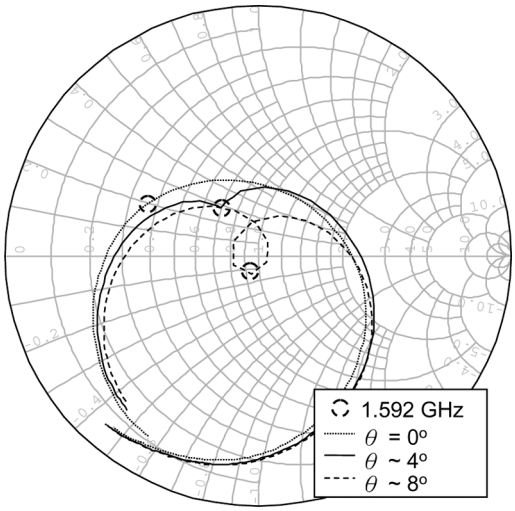

Fig. 11. The measured impedances with different rotational angles.

sponding impedance curve changes monotonously, as predicted in the simulation (Fig. 8). The antenna with the best circular polarization, where the axial ratio is 0.8 dB, is measured when the rotational angle is 4°, where a tip at the center frequency of 1.592 GHz forms in the impedance curve. The shift of resonant frequency and the required rotational angle is mainly due to manufacturing tolerance of ceramic permittivity and metal printing. When the rotational angle is increased to 8°, a circle rather than a tip occurs in the curve near the center frequency. Under this condition, the impedance bandwidth widens at the expense of degraded circular polarization; this is tradeoff between circular polarization quality and impedance bandwidth. Additionally, the center frequency remains the same with different rotating angles (Fig. 11). The self-phasing method used is convenient for tuning circular polarization without changing the center frequency.

Fig. 12(a) presents a photograph of the finished antenna, and Fig. 12(b) depicts the measured radiation pattern at 1.592 GHz with a 4° rotational angle. The radiation pattern is measured using an RHCP standard antenna. The hemispherical pattern is

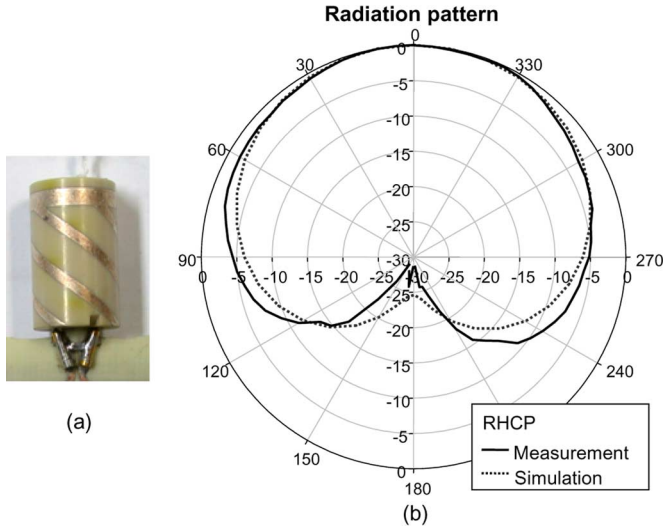

Fig. 12. (a) Photograph of the realized antenna. (b) Measured and simulated radiation patterns with normalized plots. The directivity of the realized antenna is about 2.3 dBic.

omni-directional in the horizontal plane and agrees with that simulated. The 3-dB axial ratio bandwidth is 8 MHz. The measured peak gain is -4.3 dBic including the loss of the matching network and balun, and the measured directivity is estimated as 2.3 dBic, a little lower than the simulated one (2.7 dBic), by considering the similar and wider radiation pattern as compared to the simulated pattern. The total antenna efficiency is thus about 22%. The measured 3-dB beamwidth is 150°, which performs like a hemisphere and is sufficiently wide for practical applications.

VI. Conclusion

This work presents and demonstrates the feasibility of a novel miniaturized QHA. A hemispherical circular-polarized radiation pattern and reasonable gain were achieved. The proposed self-phasing method for achieving circular polarization was flexible when tuning the axial ratio while retaining the same resonant frequency. Experimental results agree well with simulation results. The differential signal for antenna feeding can be provided by a LC balun or a differential amplifier. The small input resistance of the miniaturized QHA has been matched successfully via a simple structure without occupying additional area. Both the feeding and matching structures are quite small, low cost and simple to manufacture, and easily integrated into circuit boards. The proposed compact antenna is appropriate for mobile applications.

References

[1] R. Bricker and H. Rickert, "An S-band resonant quadrifilar antenna for satellite communication," in *Proc. IEEE AP-S Int. Symp.*, Jun. 1974, vol. 12, pp. 78–82.

[2] C. Kilgus, "Resonant quadrafilar helix," *IEEE Trans. Antennas Propag.*, vol. 17, no. 3, pp. 349–351, May 1969.

[3] M. Amin and R. Cahill, "Compact quadrifilar helix antenna," *Electron. Lett.*, vol. 41, pp. 672–674, Jun. 2005.

[4] P. K. Shumaker, C. H. Ho, and K. B. Smith, "Printed half-wavelength quadrifilar helix antenna for GPS marine applications," *Electron. Lett.*, vol. 32, pp. 153–154, Feb. 1996.

[5] J. C. Louvigne and A. Sharaiha, "Synthesis of printed quadrifilar helical antenna," *Electron. Lett.*, vol. 37, pp. 271–272, Mar. 2001.
[6] D. K. C. Chew and S. R. Saunders, "Meander line technique for size reduction of quadrifilar helix antenna," *IEEE Antennas Wireless Propag. Lett.*, pp. 109–111, Jan. 2002.
[7] A. Sharaiha and C. T. P. Blot, "Printed quadrifilar resonant helix antenna with integrated feeding network," *Electron. Lett.*, vol. 33, pp. 256–257, Feb. 1997.
[8] G. Nicolaidis, O. Leisten, and Y. Vardaxoglou, "Measurement of dielectrically loaded antennas for mobile phone handsets," presented at the ARMMS, Worcester, U.K., Nov. 23–24, 1998.
[9] G. Nicolaidis, O. Leisten, and J. C. Vardaxoglou, "TLM investigation of dielectric loaded bifilar personal telephone antennas," in *Proc. Nat. Conf. Antennas Propag.*, Apr. 1999, vol. 461, pp. 16–18.
[10] O. Leisten, J. C. Vardaxoglou, P. McEvoy, and R. S. Wingfield, "Miniaturised dielectrically-loaded quadrifilar antenna for global positioning system (GPS)," *Electron. Lett.*, vol. 37, no. 22, Oct. 2001.
[11] O. Leisten, "Dielectrically-Loaded Antenna," U.S. 6914580., Jul. 5, 2005.
[12] S.-J. Chung and Y.-S. Wang, "Antenna," U.S. Patent 7002530 B1, Feb 21, 2006.
[13] Murata Manufacturing Co. [Online]. Available: http://www.murata.com)

Yu-Shin Wang was born in May 1981 in Taichung, Taiwan, R.O.C. He received the B.S.E.E. and Ph.D. degrees from National Chiao Tung University, Hsinchu, Taiwan in 2003 and 2008, respectively.

His research interests include antenna equivalent circuit model and small antenna design. He is currently with Teradyne, Inc., Hsinchu, Taiwan, R.O.C., and has research in the field of interconnection design and signal integrity.

Shyh-Jong Chung (M'92–SM'06) was born in Taipei, Taiwan, R.O.C. He received the B.S.E.E. and Ph.D. degrees from National Taiwan University, Taipei, Taiwan, R.O.C., in 1984 and 1988, respectively.

Since 1988, he has been with the Department of Communication Engineering, National Chiao Tung University, Hsinchu, Taiwan, R.O.C., where he is currently a Professor. From September 1995 to August 1996, he was a Visiting Scholar with the Department of Electrical Engineering, Texas, A&M University, College Station. He has authored or coauthored over 70 technical papers in international journals or conferences including several invited papers and speeches. His areas of interest include the design and applications of active and passive planar antennas, communications in intelligent transportation systems (ITSs), LTCC-based RF components and modules, packaging effects of microwave circuits, and numerical techniques in electromagnetics.

Dr. Chung serves as the Chairman of IEEE MTT-S Taipei Chapter from 2005. He was also the Treasurer of IEEE Taipei Section from 2001 to 2003.